Proceedings of the International Conference on Aerospace Science and Technology
26-28 June 2008, Bangalore, India

INCAST 2008-044

DESIGN OF SPAR SPLICE JOINTS IN COMPOSITE WING STRUCTURES

Polagangu James [1], Gaddikeri Kotresh [2], D. Murali Krishna [3],
B. Ramanaiah [4], Byji Varughese [5], M. Subba Rao [6]

[1] Advanced Composites Division, National Aerospace Laboratories, Bangalore, India, james@css.nal.res.in
[2] Advanced Composites Division, National Aerospace Laboratories, Bangalore, India, kotresh@css.nal.res.in
[3] Advanced Composites Division, National Aerospace Laboratories, Bangalore, India, dmkrishna@css.nal.res.in
[4] Advanced Composites Division, National Aerospace Laboratories, Bangalore, India, ramanaia@css.nal.res.in
[5] Advanced Composites Division, National Aerospace Laboratories, Bangalore, India, byji@css.nal.res.in
[6] Former Head of the Division Advanced Composites Division, National Aerospace Laboratories, Bangalore.

ABSTRACT: *Mechanically fastened splice joints like spar splice joints are essential in a large aircraft structure like wing to join inboard and outboard pieces spar members. Typically in a spar splice joint the inboard and outboard pieces of the spars are mechanically joined using splice plates. Such a splice joint often transfers large shear loads associated with bending moment and the joint behaviour is complex. In this paper the design procedure of a spar splice joint in a Carbon Fibre Composite (CFC) wing for a light transport aircraft is presented. The methodology of design in the preliminary design stage and the design validation with an element level test are discussed. Conventional strength of materials approach of the mechanically fastened joints is quite extensively used in the design. The fastener configuration at the splice joint location is decided based on standard design practices of web splice joints that are subjected to bending and shear loads. The fastener loads at different levels along height or span are then computed based on the linear distribution of bending strain and parabolic distribution of shear stress at the splice joint. The distribution of forces among the fasteners at each level is estimated based on fairly reasonable considerations of fastener pattern. This approach is quite novel compared to the conventional way of equally distributing the shear force and bending force. The design has been validated subsequently with static test on a spar splice specimen that has all the essential features of the splice joint in the wing. The various constraints in synthesizing the design of test specimen (which is an open section) to nearly simulate the wing (which is a closed box) are discussed. The splice joint specimen was subjected to the shear force that is seen in the wing. The specimen safely withstood the design ultimate load. The strains on the specimen at crucial locations were monitored during test. These strains have shown good correlation with the strains predicted from classical analysis. The testing of spar splice joint is an important step towards the certification programme.*

1. INTRODUCTION:

A large aircraft structure like wing is often made in multiple pieces like outboard and inboard or centre piece to achieve many advantages in fabrication and assembly to the fuselage structure. These pieces are joined through mechanically fastened splice joints on the primary load carrying members like spars, top skin and bottom skin. In a typical skin splice joint the top skin and the bottom skin of inboard and outboard pieces are spliced at a rib location. In a spar splice joint the inboard and outboard pieces of the spars are mechanically joined using splice plates. In a wing structure much of bending moment is resisted by the skins and shear force is resisted by the spars. Hence, the splice joints in skins and spars are designed for these forces. The importance of the joint design in the preliminary stage of the programme was brought out in a previous paper [1]. In this paper the design procedure of a spar splice joint in a Carbon Fibre Composite (CFC) wing for a light transport aircraft is presented. The methodology of design in the preliminary design stage is discussed. The validation of the spar splice joint design is done using a splice joint specimen that has all the relevant features of the joint in the wing. The

details of the test results and their correlation with results predicted from the design are discussed. The testing programme fills up the requirement of element level testing in the building block approach.

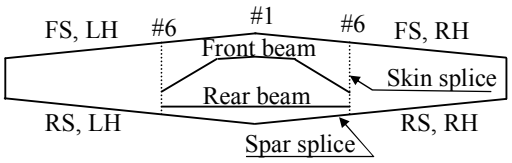

Fig-1: Lay out of the wing

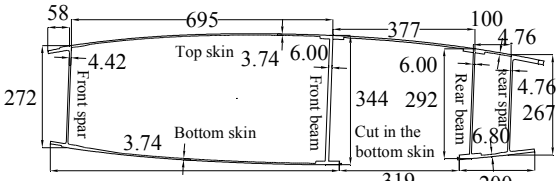

Note: Units are in mm

Fig-2: Cross section of the wing at splicing

2. GEOMETRY DETAILS:

The composite wing has a span of 14 m. Since there are a few specific advantages in fabrication and assembly of the wing to the fuselage, the whole wing is divided into three pieces: two out board pieces and one centre piece. The centre piece is from station#6 of left hand (LH) wing to station #6 of right hand (RH) wing. The outboard pieces are from station #6 to station #23 of the LH and RH wing. The wing has two spars; a front spar (FS) and a rear spar (RS). These details are shown in Fig-1. Figure shows the plan view of the interspar (I/S) box. Top and bottom skins of centre and outboard pieces are spliced at station #6. The front spar and rear spar are spliced between station #5 and station #6 of the LH and RH wing. There is a main landing gear (MLG) cut out in the bottom skin between station # 1 and station # 6. There are two beams a front beam and a rear beam from station #6 LH and station #6 RH. The beams surround the MLG cut out. A typical cross section of the wing very close to the spar splice location is shown in Fig-2. The locations of front spar, front beam, rear beam, rear spar and MLG cut out in bottom skin can be seen in Fig-2. The cross section of front spar and rear spar are of inverted J-shape. The beams are of I-section.

3.0 DESIGN OF SPAR SPLICE JOINT

In order to carry out the design of the splice joint it was required to understand the bending stress and shear stress distributions at the splice location. The following section.3.1 and section.3.2 explain how the bending stress and shear stress values at each row of fasteners are determined.

3.1. Bending stress distribution in skins of wing:

For design of top and bottom flange of spar splice plates, it is required to know the bending stress distribution in top and bottom skins respectively. The bending stress distribution in skin members is determined based on available theoretical methods. Initially it is assumed that there is no cut out in the bottom skin. A complete gross section of the wing is assumed as shown in Fig-3. The exact moment of inertia of the wing section has been calculated using soft tools, which reduce the error in calculating the second moment of area. The distance of top and bottom skins about neutral axis position is also shown in Fig-3. The basic bending stresses distribution (without considering the cut out in bottom skin) in skin members are shown in Fig-4.

Since there is no cut out in the top skin, no correction factors are applied to the basic bending stress distribution in the top skin. A correction factor to the bending stress distribution to the effect of huge cut in the bottom skin has been applied. This correction factor increases the bending stress value in the bottom skin, which is representative stress distribution in the bottom skin member. In bottom skin the first row of values shows the basic bending stress values. Second row of values shows the additional increased bending stress values due to presence of cut out in the bottom skin. Third row of values shows that the correction made to the second row of values considering the effect of the height of the web members in Box-1 and Box-2 as shown in Fig-4. The final bending stress value in the bottom skin is given against fourth row, is the sum of first and third row of values.

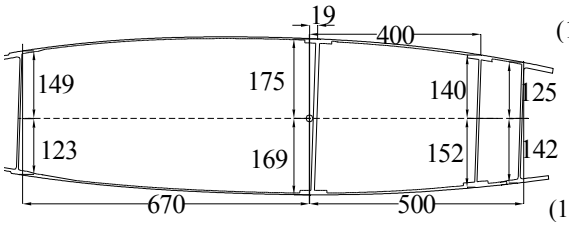

Fig-3: Gross cross section

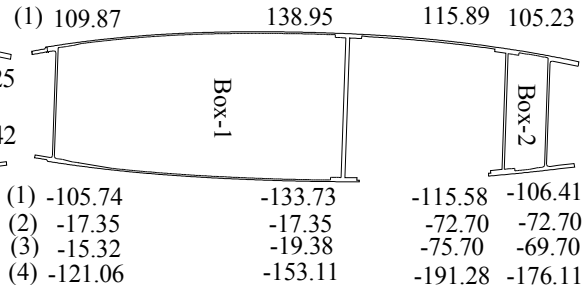

(Note: Units are in mm, MPa)

Fig-4: Bending stress distribution

3.2. Shear flow distribution in web members:

For design of web portion of spar splice plates, it is required to know the shear flow distribution in the web of spars. Shear flow distribution in the wing section having multiple cells can be determined using available mathematical techniques. The particular cross section of the wing under considered shown in Fig-4 does not fall under the category of multiple cells. The peculiarity in the cross section of wing is the huge cut out in the bottom skin. Hence the present theories on shear flow distribution calculation may not be applicable for this problem. Therefore it is felt at this level of understanding that additional mathematical techniques are required that account the effect of cut out in the bottom skin between rear beam and rear spar as shown in Fig-2. Up on carrying out the shear flow analysis on outboard portion of the wing (without considering the contribution of nose box and aft box), the shear force acting in front spar is about 45%, in rear spars it is about 55%. These percentage values of shear force is valid only in the portion of wing extended between station #6 and station #23 where the additional shear resisting members (front beam and rear beams) are not present. In spite of knowing the fact that introduction of additional shear resisting members in *inboard* of the wing causes sudden change of shear flow distribution in front spar and rear spar. The shear flow distribution shown in Fig-5 is determined approximately based on certain assumptions. However that work has not been presented in this paper. It is observed from shear flow analysis of the section shown in Fig-5, the total shear force acting in the rear spar is 44082 N upwards. This value is less than that of 55% of 127844 N total shear force acting at the splicing point in the wing structure.

In absence of exact mathematical techniques cited in above paragraph, it is assumed that the shear force acting in front spar and rear spars of inboard wing as same percentage (45% in front spar and 55% in rear spar) as that of outboard portion of the wing which is conservative. Therefore, the total shear force acting in the rear spar of the wing is assumed not less than 55% of 127844 N, i.e. 70314 N. The shear flow distribution in the rear spar shown in Fig-5 is true when 44082 N of shear force is acting in it. But it is assumed that the shear force in rear spar is equal to 70314 N, which will makes the values given in rear spar in the same figure is to be increased by 1.595 times to cater for the shear flow distribution in rear spar of 70314 N. The geometrical configuration of fasteners and cross section at the center of splicing is shown in Fig-6 and Fig-7 respectively. Knowing the shear flow distribution in the rear spar the total vertical force due to vertical shear is calculated at the level of each row of fasteners. In conventional design methods, it is assumed that total vertical shear force is equally shared by the total number of fasteners in a given column or row of fasteners. These assumptions are not followed in the present problem, as it may not take care of the actual distribution of shear flow in the web of the spar. The distribution of shear force due to bending stress and shear stress among all fasteners in a given row or column is discussed in Section.4, subsequently the design of splice plates is discussed in Section.5

4. DETERMINATION OF RESULTANT SHEAR FORCE IN FASTENERS:

The resultant shear force acting in the fasteners under consideration consists of two components. First of which is the horizontal component of shear is due to the bending stress acting in the direction of bending stress resultant. The second of which is the vertical shear force acting in the direction of vertical

shear force. The properties of material used for fabrication of wing are given in Table-1. The lay-up sequence and thickness of each structural component considered is given in Table-2. For the given lamination sequence, determination and distribution of shear force among all fasteners available at the splice joint are dealt with separately in the following sections.4.1 and section.4.2.

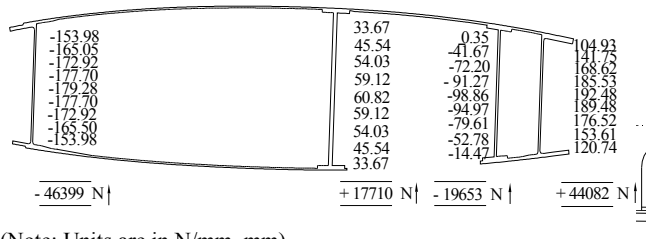

(Note: Units are in N/mm, mm)

Fig-5: Shear flow distribution in the wing

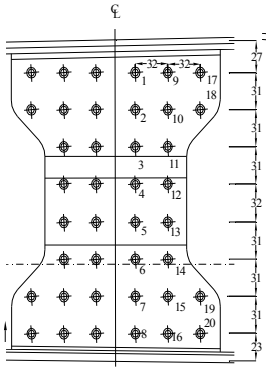

Fig-6: Fastener configuration

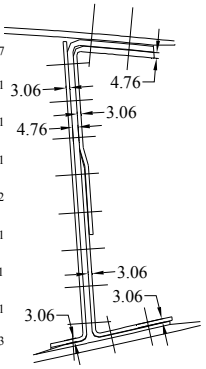

Fig-7: Cross section

Table-1: Material properties

Property	Allowables	
Tensile strength (X_T)	585	MPa
Compressive strength (X_C)	494	MPa
Shear strength (G_{LT})	46	MPa
Modulus in fiber direction	130	GPa
Modulus in transverse direction	8	GPa
Shear modulus (G_{LT})	3	GPa
Poisson's ratio (υ_{LT})	0.32	
Thickness of lamina	0.17	mm
Density	1.5	g/cc

4.1. Determination of shear force due to bending moment:

The structural component available in the wing at point of splicing prior to the spar splicing are considered as prime structural components to resist the induced bending moment and shear force. Knowing the variation of bending stress values in skin members as shown in Fig-4, the resultant stress per unit width (N/mm) is calculated by multiplying the stress value with the corresponding thickness of skin members. The strain values in top skin of 1980 Microstrains and bottom skin of 2100 Microstrains along the span of the wing (along '0' ply direction) are determined. Linear variation of stress from top skin to the bottom skin can not be assumed in composite material due to its orthotropic property. The strains are assumed to vary linearly from top skin to bottom skin. Based on which the strain values at each row of fasteners are determined as shown in Fig-8. The strain values obtained thus are then multiplied by effective Young's modulus 'E_1' of laminate in the web of spar in '0' ply direction along the span to get the stress values in the web of spar as shown in Fig-9. Once the stress distribution in the web of spar is known, the total shear force acting at each row of fasteners as shown in Fig-10 can be determined by multiplying those stresses with cross section of the web of spar for a given spacing (thickness x vertical spacing).

4.1.A. Distribution of shear force due to bending moment:

In this design it is assumed that all fasteners in a given row will not share equal amount of horizontal force when subjected to horizontal shear force. Assumptions are made in the present work to distribute

shear force due to bending moment in a given row so that the fastener forces are conservative. Refer to Fig-10, 1). In case the numbers of fasteners in a given row are 3, the fastener which is near to the splice line attracts about 60% of total force in a given row. The middle one shares about 15 % of total force, and the fastener far from the center of splicing shares about 25% of total force. 2). In case the number of fasteners in a given row are 2, the fasteners which is near to the center of splicing attract about 60 % of total horizontal force, and that fastener far from the center of splicing attracts about 40 % of total horizontal force. The same distribution of shear force in a given row is also valid in top and bottom flange as shown in Fig-13.

Table-2: Lay-up sequence of laminates available at the center of spar splicing

Name of the structural Components	Thickness (mm)	No of layer	Lay-up sequence
Top skin	5.10	30	(+45, -45, 0, 90, 45, 0, 90, -45, 0, 90, 45, 0, -45, 0, 90) Sym
Bottom skin	6.80	40	(+45,-45, 0,0,+45,0,0,90,0,0,-45,0,0,+45,0,-45, 0,0,90, 0) Sym
Top flange of the spar	4.76	28	(+45, -45, 0, +45, 0, 90, -45, 0, +45, 90, -45, 0, 90, 0) Sym
Web of the spar	4.76	28	(+45, -45, 0, +45, 0, 90, -45, 0, +45, 90, -45, 0, 90, 0) Sym
Bottom flange of the spar	2.72	16	(+45,-45,0,+45,0,90,-45,0,+45,90,-45,0,90,0,-45, +45)Total
Top flange of splice plate	4.76	28	(+45, -45, 0, +45, 0, 90, -45, 0, +45, 90, -45, 0, 90, 0) Sym
Web of splice plate	3.06	18	(+45, -45, 0, +45, 90, 0, –45, 0, 90) Sym
Bottom flange of the splice plate			
a) Test specimen	2.72	16	(+45,-45,0,+45,0,90,-45,0,+45,90,-45,0,90,0,-45,+45) Total
b) Wing	3.06	18	(+45, -45, 0, +45, 90, 0, –45, 0, 90) Sym

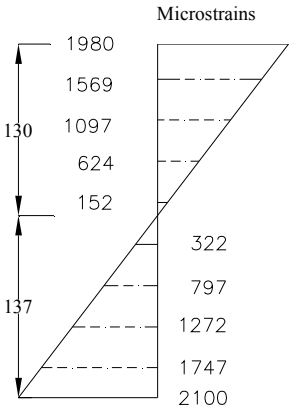

Fig-8: Bending strain distribution

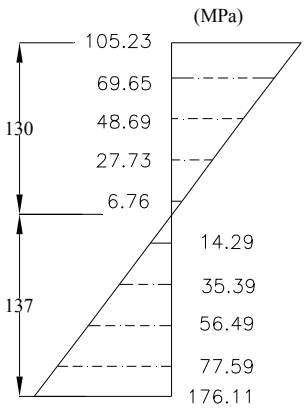

Fig-9: Bending stress distribution

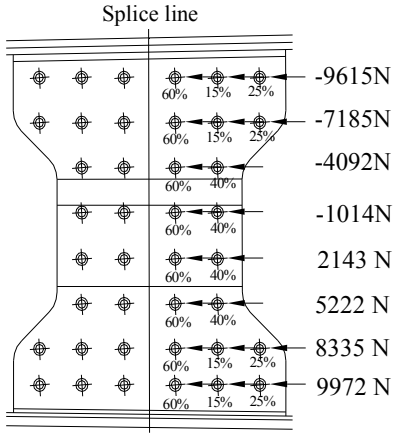

Fig-10: Percentage distribution of shear force due to bending

4.2. Determination of shear force due to shear flow distribution:

The shear force acting in the rear spar is assumed as 55% of total shear force acting at that section as already explained in section.3.2. Subsequently, the shear flow is multiplied by the center to center spacing of fasteners along the direction of the flow to get the total reacting shear force acting at each row of fasteners as shown in Fig-11.

4.2.A. Distribution of shear force due to shear flow:

In conventional design methods it is assumed that all fasteners share equal amount of vertical shear force. In this study it is assumed that all fasteners in a given row share vertical shear force based on parabolic distribution of shear force. Refer to Fig-11, 1). In case the numbers of fasteners in a given row are 3, the fastener which is near to the center of splicing attracts about 25% of total force in a given row. The middle one shares about 15 % of total force in a given row, and the fastener far from the center of splicing shares about 40% of total force in that row. 2). In case the number of fasteners in a given row are

2, the fasteners which is near to the center splicing attract about 40 % of total vertical force, and that fastener far from the center of splicing attracts about 60 % of total vertical shear force in a given row. The percentage of distribution is also valid in top and bottom flange of the section under consideration is as shown in Fig-12.

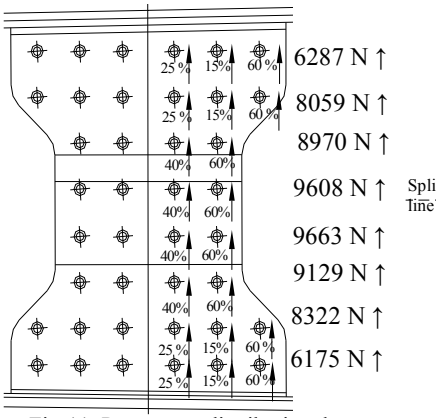

Fig-11: Percentage distribution due to vertical shear

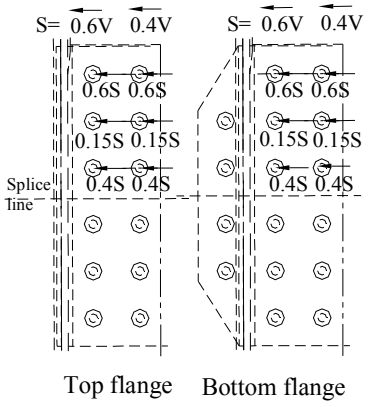

Fig-12: Shear due to shear distribution in the flanges

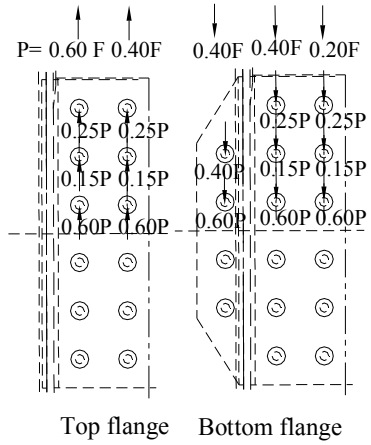

Fig-13: Shear due to bending distribution in the flanges

Note: V=Shear force in the flange due to shear flow distribution, F=Axial force in the flange due to bending stress

5. DESIGN OF SPLICE PLATES OF REAR SPAR:

For design of composite laminate especially at splicing location it is required to know the shear force acting in the critical fastener used in it. Following the distribution of shear force due to bending stress and shear force discussed in the above sections, the resulting shear force in each fastener available at the spar splice have been determined. Thickness of each laminate has been arrived at in such way that the margin of safety in bearing is the least when compared with other modes of failures. The thickness of each laminate of splice plates is shown in Fig-7. The lamination sequence of the splice plates are given in Table-2.

6.0. VALIDATION OF DESIGN THROUGH TESTING:

It is observed from Fig-4, the maximum stressed component in the wing is the bottom skin extended between rear beam and rear spar. The most critical section that needs to be considered for the purpose of testing is the section between rear beam and rear spar.

6.1. Design of test specimen:

The geometry of test specimen along the span is shown in Fig-14-(a). The cross sectional detail of test specimen at the center of splicing is shown in Fig-14-(b). The design of test specimen was carried out to meet the following requirements.

1. The test specimen should represent the thickness and lay-up sequence of corresponding laminate available at the splice joint in wing structure.

2. In wing structure the rear spar of inverted ‘J’ section. If this section is used for testing then the load has to be applied through the shear centre to eliminate the twisting of specimen. This involves the design of special loading fixtures. However, the wing section is a closed box and torsionally very stiff and the twist is minimum under the applied loads. This condition is simulated by making the inverted ‘J’ section in to symmetric ‘I’ section about its vertical plane.

The load was applied through the centre of the web to avoid twisting, thus indirectly simulating the wing torsional rigidity.

3. Upward load P_1 and downward load P_2 are applied to keep the constant bending moment between P_2 and fixed support so that the skin thicknesses at the fixed end connection are as minimum as possible. The test specimen is fixed at one end and submitted to a two point loads each of 67369 N, the distance between these two point loads is 629mm. The loading system applied on test specimen induces pure shear between point load P_1 and P_2, and zero shear force between fixed end and point load P_2. It induces varied bending moment between point load P_1 and P_2, and pure bending moment between point load P_2 and fixed end.

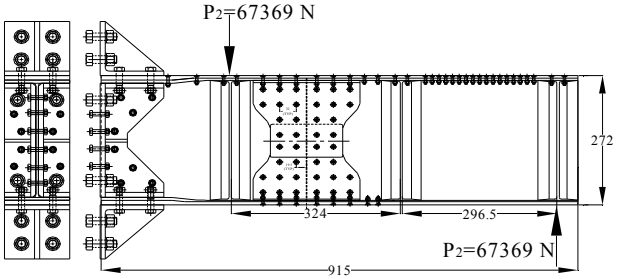

Fig-4-(a): Spar splice test specimen

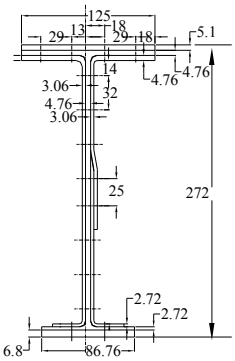

Fig-14-(b): Cross section of specimen at the center of splicing

6.2. Testing of the specimen:

The assembled spar splice test specimen when mounted on test rig, along with strain gauges and dial gauges are shown in Fig-15-(a). The specimen was strain gauged extensively to capture the structural response. A few strain gauges of interest considered for comparison of measured strains with estimated strains are shown in Fig-15-(b). The specimen was loaded and unloaded in steps of 10% of design ultimate load and strains and deflections were recorded. The specimen withstood the design ultimate load successfully without any failure. No residual strains were observed after unloading.

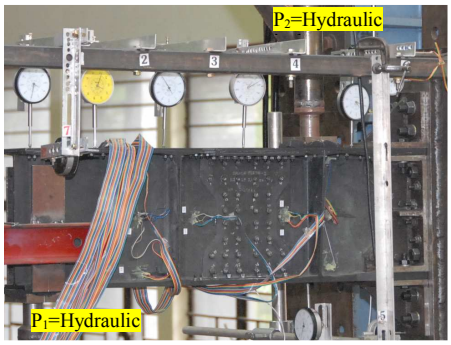

Fig-15-(a): Photographic view of the spar splice test specimen mounted on test rig

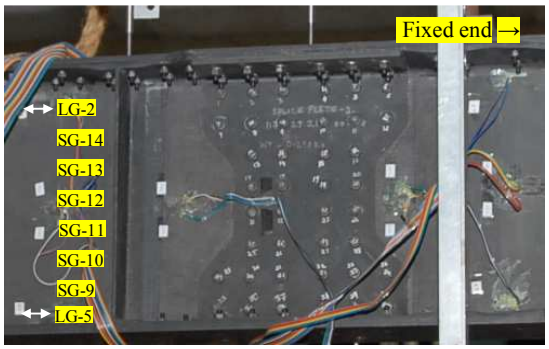

Fig-15-(b): Location of strain gauges considered for comparison of strains with design values

6.3 Estimation of strains from classical lamination theory:

An infinitesimal element as shown in Fig-16 has been considered at strain gauge locations shown in Fig-15-(b). The bending stress value at respective location is applied as an axial compressive / tensile

stress along with shear stress at that location as complementary shear stress are applied on this infinitesimal element. The axial and shear strains are computed at each location of strain gauge using classical lamination theory [2, 3]. The strain values estimated as above and measured from the test results are given in Table-3. It is observed from these strain values that the design strains values are in good agreement with measured strains. After the test the specimen was dismantled and inspected for damage. It was observed that there were no delamination, no elongation of holes and no bending of fasteners.

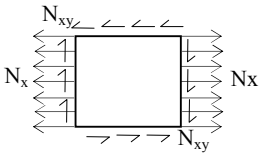

Fig-16: Infinitesimal element subjected to axial and complementary shear stress

Note: Refer Table-3. The gauges LG-1 and LG-6 are placed opposite to LG-5 and LG-2 respectively. The difference in measured strain values of these gauges is attributed to the minor eccentricity of applied load with respect to shear centre.

Table-3: Comparison of estimated strain (CLT) with measured strain values at DUL

Strain gauge Number	Applied (N/mm)			Estimated Strain (CLT)	Measured Strain values	% of error in strain values
	N_x	N_y	N_{xy}			
LG-2	-196.87	0	+233.55	-688	-878	-27.6%
LG-6	-196.87	0	+233.55	-688	-516	24.6%
SG-14	-120.05	0	+266.29	-1884	-2064	-9.5%
SG-13	-120.05	0	+266.29	+1602	+1774	-10.7%
SG-12	-13.66	0	+280.73	-1854	-1927	- 3.9%
SG-11	-13.66	0	+280.73	+1822	+1924	-5.6%
SG-10	+92.34	0	+257.38	-1576	-1651	-4.8%
SG-9	+92.34	0	+257.38	+1793	+1848	-3.1%
LG-1	+173.07	0	+217.20	+605	734	-21.3%
LG-5	+173.07	0	+217.20	+605	632	-4.5%

7. CONCLUSION:

The splice joint is designed after accounting the effect of cut out in the bottom skin due to main landing gear. The spar web and splice plates are designed by keeping the margin of safety minimum in bearing. The distribution of force in the fasteners is assumed to be conservative while sizing the splice plates and fasteners. The resulting spar splice joint is tested on a stand alone test specimen up to the design ultimate load. The specimen successfully withstood the ultimate load without any failure. This indicates the efficacy of the design. The strains estimated from classical laminate theory are in good agreement with the measured strain values.

ACKNOWLEDGEMENT:

Authors wish to thank the Director of National Aerospace Laboratories for his unstinting support during this programme and our colleagues Ramesh Sundaram, GopalaKrishna M Kamath, Ramachandra H V, Sanjeev Kumar S, and B L Dinesh for the support given during the various stages of this work.

REFERENCE:

[1]. D. Murali Krishna, B. Ramanaiah, Polagangu James, Kotresh M. Gaddikeri, Byji Varughese., M. Subba Rao "Experimental Investigation on a Mechanically Fastened Splice Joint in Composite Aircraft Wing," *National Seminar on Aerospace Science (NASAS),* October, 2007,Coimbattore , TN, India.

[2]. H. Altenback, J. Altenbach, W. Kissing "Mechanics of composite structural Elements," June 2003, *Springer publication*, Germany.

[3]. Robert M. Jones "Mechanics of composite Materials," Second Edition, April 1999, *Taylor & Francis Inc,* Philadelphia.